From electrical resistivity to Volumetric Water Content tomographies: how to optimize irrigation in horticulture

A. Innocenti[1], R. Fanti[1] , V. Pazzi[1]

[1] *Department of Earth Sciences, University of Florence, Italy*

Introduction

Water plays a key role in agriculture: irrigated soils account for about 20% of cultivated land (Wanniarachchi and Sarukkalige, 2022). Thus, agricultural water management is becoming an increasingly actual issue in a period of severe climate changings. Sustainable water management requires adequate knowledge of soil water availability and its storage capacity (Chartzoulakis and Bertaki, 2015). Researchers and farmers focus on irrigation scheduling, assessing when and how much to irrigate. The optimal timing depends on factors such as crop growth, water stress, and water availability. Additionally, the irrigation method, i.e., how water is applied to the soil, is crucial for effective water management (Ratke et al., 2023).

Nowadays, the drip irrigation method, often associated with the film mulching ridge, is among the most widely used and most effective for water management in agriculture (Arshad, 2020). This system prevents water loss through spraying and improves soil surface temperature (Zhang et al., 2022). The mulch ridge is created where surface drainage is not installed and allows the water table to be lowered, preventing surface water stagnation, and encouraging the water flow towards collection ditches, generally positioned along the edges of the field. The ridge is made by specific plowing that creates a convex surface profile with a slope that depends on the terrain type, generally in the range 1-3 % (Luo et al., 2023). The correct management of the drip system in a horticultural context where film mulching is used requires a good knowledge of the volumetric water content (VWC) in the soil. VWC is a parameter that can be measured using soil humidity sensors, and it can help understanding how the irrigation water distributes in the soil (Ratke et al., 2023). However, these sensors are just point humidity monitoring systems, that means they provide information limited to the vertical where they are installed and do not allow a 2D or 3D reconstruction of the water content in the subsoil.

Electrical Resistivity Tomography (ERT), a well-known geophysical method, are often used in groundwater research (Acosta et al., 2022). This method, in fact, can estimate the spatial and temporal variations of soil conductivity, which is linked to parameters such as water content, soil-root interactions, salinity, temperature, and soil texture (Vanella et al., 2021). In contrast to point-type soil moisture sensors, ERTs provide a spatial view of soil water distribution. Thus, the goals of this study were to evaluate the effectiveness of the two- and three-wings drip irrigation system associated with the mulch cover of different heights, and to reconstruct the VWC subsoil distribution by full 3D-ERT and humidity sensors. This research seeks to enhance irrigation management and optimize water resource use in horticulture, minimizing waste while ensuring optimal conditions for crops.

Method

The survey campaign was carried out in an agricultural field used for the cultivation of melons (Cucumis melo) in Barbaruta (42.804113° N, 11.02322° E; 19 m a.s.l.), in the municipality of Braccagni (Grosseto, Tuscany - Italy, Figure 1). To achieve the specific goals mentioned in the Introduction, full 3D-ERTs surveys were collected in two different fields and in two different melon growing periods (April-June 2023 and June-August 2023). In this work, only the results obtained during in the latter period are presented (for more details see Innocenti et al., 2024b).

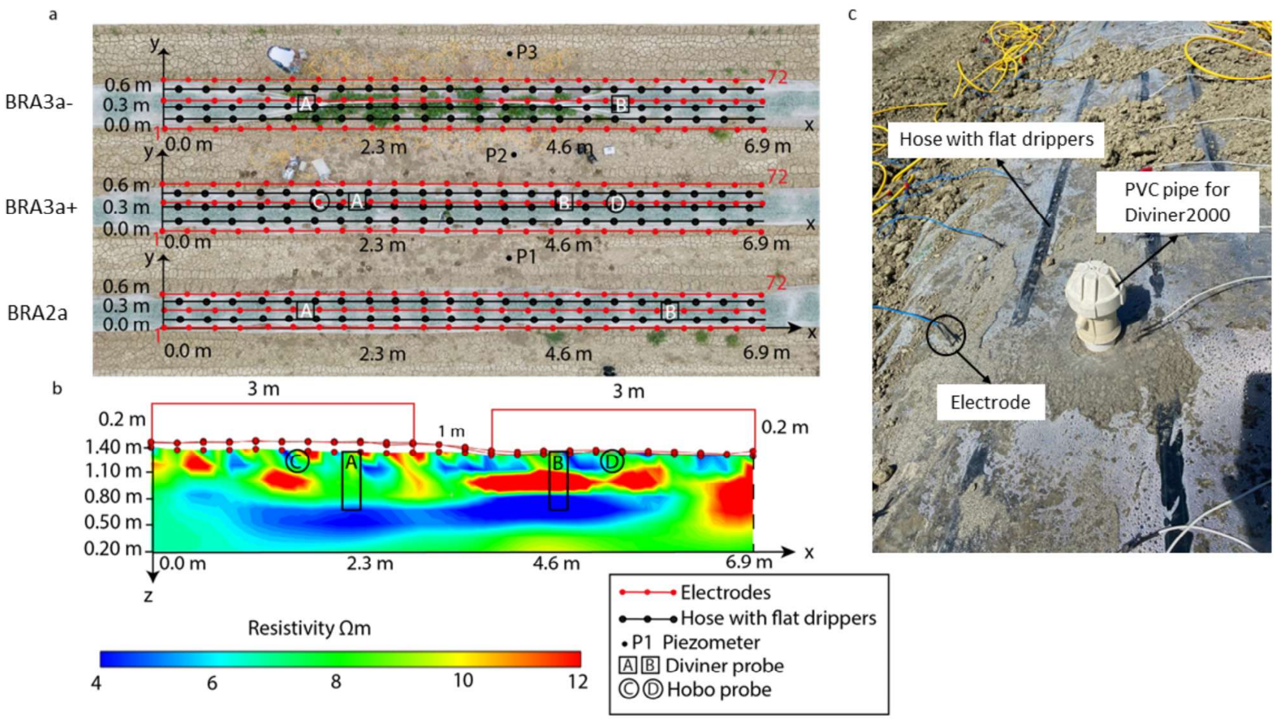

Fig. 1 a) Experimental set-up of the study site with the position of the 3 layout (from the top to the bottom: BRA2a, BRA3a+, and BRA3a-), the electrodes (red), the hoses with flat drippers (black), the Diviner2000 sensors (indicated with the square and the letter A and B), the ECH20 10HS sensors (indicated with the circle and the letters C and D), the piezometers (P1, P2, and P3). b) ERT example where is visible the different high of the mulching ridge. c) Photo of the ERT profile detail along a row of melons and PVC pipe for Diviner2000 probe.

Data ERTs were acquired using a 10-channel SyscalPro receiver (Iris, Orléans, France), with 72 electrodes arranged for full 3D data acquisition. Three 3D-experimental set-ups were deployed along three adjacent plots of the same field (Figure 1a). The electrode set up was optimised during a campaign in summer 2021 and fully applied in summer 2022 (Innocenti et al., 2004a). The results of the 2022 campaign are described in detail in Innocenti et al., (2024a). Specifically, each ERT layout is made of 72 electrodes arranged in 3 parallel lines of 24 electrodes each (red dots in Figure 1a). The investigation area of each layout has a length of 6.9 m and a width of 0.60 m. Electrodes are AISI 316 stainless steel bars, 0.20 m long and with a diameter of 5 mm. Each electrode was driven into the ground for approximately half of its length (Ciani et al., 2024) and spaced 0.30 m both between electrodes and lines, and reaching an investigation depth of approximately 1.20 m, using the dipole-dipole array configuration. They were installed in June 2023 and left in place until the end of the acquisition of the measurements.

The difference among the 3 layout is the drip irrigation system (black dots in Figure 1a). One was set up with a 2-wings drip irrigation system (BRA2a at the bottom of Figure 1a) with a flow rate of 4.1 lh/m^2, the second was set up with a 3-wings drip irrigation system (BRA3a+, in the middle of Figure 1a) and a flow rate of about 5 lh/m^2, and finally the third (BRA3a-, at the top of Figure 1a) was set with a 3-wings drip irrigation system as BRA3a+, but with the flow rate. Each layout was divided into two parts with different heights: the left side, 3 m long, has a mulch height of approximately 0.20 m, while the right side, 3 m long too, was at ground level. The transition zone between the two heights has a length of less than 1 m, as visible in Figure 1b.

ERT data were acquired using an optimised full 3D dipole-dipole configuration that took 1.5 hours per field (see Innocenti et al., 2024b). The ERT monitoring were carried out in time-lapse mode, i.e., acquiring data at different times during the cultivation phase, just after an irrigation cycle was ended. For each layout, a measurement, defined as measurements at time 0 (T_0), was carried out before to the transplanting of the melon plants and thus before the beginning of the irrigation. It allowed to know the resistivity values of the soil without the influence of the plants roots and, above all, that of the irrigation water. A total of 11 datasets were acquired and, processed with ErtLab™ software (Geostudi Asiter) using a cubic mesh (0.15 m cells).

Soil moisture was measured using two sensors: the Diviner2000 probe and the Soil Moisture ECH20 10HS. The Diviner2000, calibrated before the use, measures water content, through a portable unit recorder, at 0.10 m intervals using PVC tubes. They must be closed at the bottom and at the top with an opening cap, and permanently installed in the field (Figure 1c). The PVC pipes have a length of 0.70 m and a diameter of 5.5 cm. Each layout was equipped with 2 PVC tubes (indicated with black square and the letters A, in the high ridge part, and B, in the zero-height ridge part, in Figure 1a). The Diviner2000 probe was slid inside these tubes with a constant speed movement during each acquisition campaign. Two HOBOnet Soil Moisture ECH20 10HS sensors were installed in correspondence with the central plot, indicated with the black circle and the letters C and D in Figure 1a, and connected to a HOBO® datalogger which records soil temperature and humidity every 30 min. The probes, having a length of 15 cm, were installed vertically in the soil, allowing the VWC measurement of 0.001 m^3 soil volume (Innocenti et al., 20024b).

The soil moisture content depends on both precipitation and irrigation. Rainwater, being almost distilled, has high resistivity, while the resistivity of irrigation water depends on its ion content. Therefore, to evaluate the effect of rainwater on resistivity, a study of precipitation was conducted using data collected from a nearby station. During the study period, no significant rainfall events were recorded (see for more details Innocenti et al., 2024b). This means that the geoelectrical and moisture measures, taken during the experimental period, are a function of the soil's conductivity and the effect of irrigation water.
To monitor the depth of the irrigation water in the soil, and calibrate the ERTs results, 3 piezometers 1.5 m long were installed. They were PVC pipes with a diameter of 5.0 cm, open at the bottom, and

sealed at the top to prevent rainwater from entering (P1, P2, and P3 in Figure 1a). Several holes were drilled on all sides of the piezometers to allow irrigation water to enter.

Results and discussion

The ERTs results show significant differences among the three plots. In the following, for brevity, only some selected ERTs results will be presented (Figure 2). In particular, the ERTs acquired at three different times (T_0, T_1, and T_6, i.e., just after the preparation of the land – Figure 2a, after the first irrigation cycle – Figure 2b, and the last acquisition – Figure 2c, respectively). BRA2a shows a clear difference between the high and low ridges, with the latter having higher conductivity values. The distribution of irrigation water is not homogeneous throughout the investigated area. It can be observed that the most conductive surfaces (the first 10 cm) are concentrated near the drippers compared to the ends of the field, and that in the low ridge, the water concentration is higher than in the high ridge. Additionally, the vertical slice corresponding to 0.60 m on the y-axis is more conductive in all the tomographies.

Of all the three systems tested, BRA3a+ shows significantly higher conductivity values. The difference between point "A" and point "B" is much less noticeable, but it can be observed that the low ridge has slightly higher conductivity values compared to the high ridge, where a greater concentration of high resistivity areas is found. These tomographies also show how the distribution of irrigation water is much more homogeneous across the entire area. This irrigation system immediately created an excessive accumulation of water below the root zone, indicated in Figure 2b-c with a dashed black line, and confirmed by the piezometer P1.

BRA3a- presents a good distribution of irrigation water, represented by the conductive zones. Again, the most conductive area is the lower ridge. The surface level between 1.04 m and 1.34 m remains quite constant over time, and the water distribution is much more homogeneous compared to the BRA2a system, despite the same amount of water being introduced. The tomographies show that this system provides a better water supply to the root system, as the downward runoff is also lower than in BRA3a+ and BRA2a, indicating less water waste.

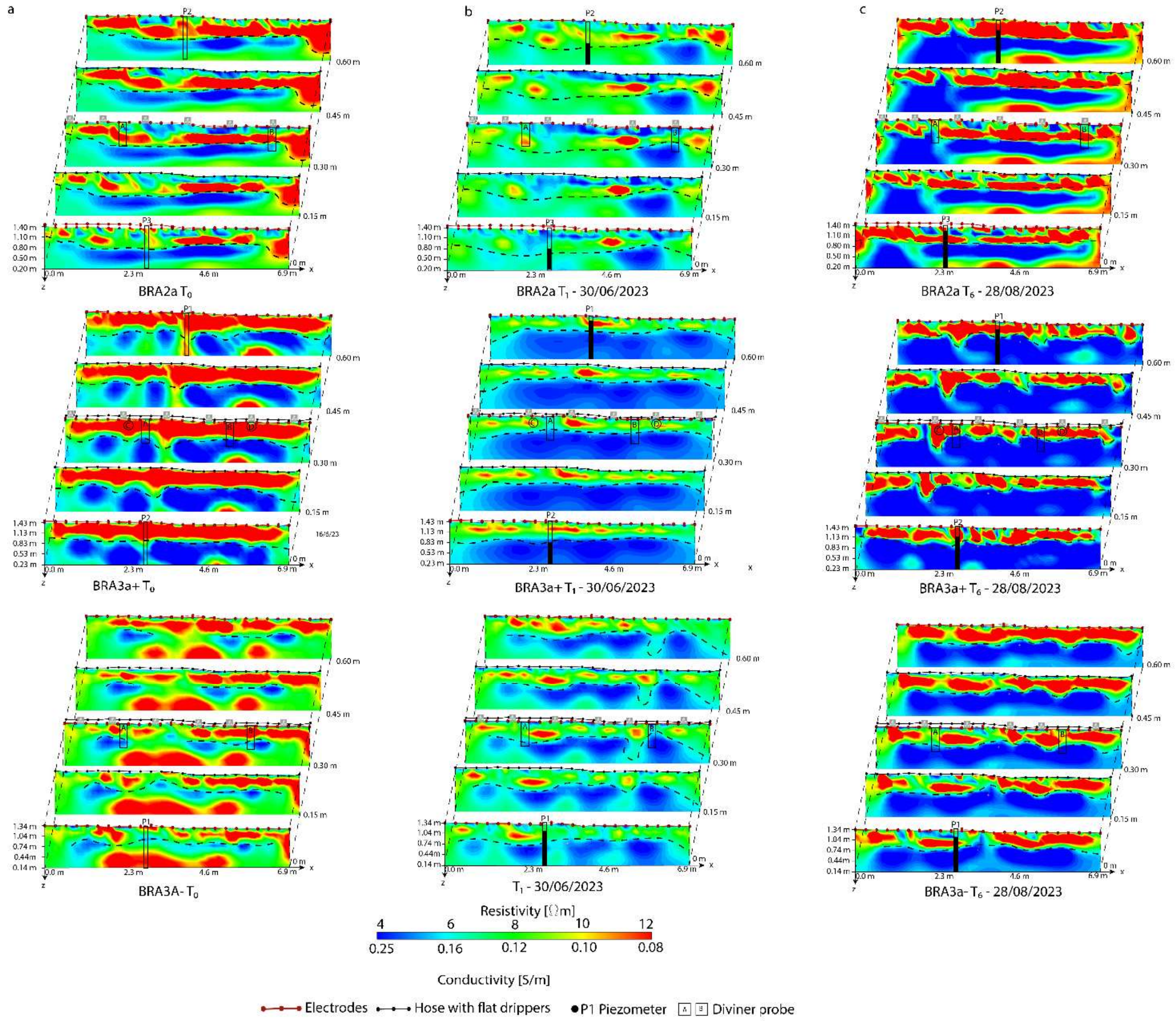

Fig. 2 – a) ERT results for BRA2a, BRA3a+, and BRA3a- at time T_0. The black dotted line represents the depth of tilled soil at this acquisition time. b) Electrical resistivity tomography campaign results BRA2a, BRA3a+, and BRA3a- at time T_1. The dashed black line represents the level of the water table. c) Electrical resistivity tomography campaign results BRA2a, BRA3a+, and BRA3a- at time T_6. The dashed black line represents the level of the water table.

The ERT results highlight a 2-layers soil stratification: the upper one more resistive, represents the mulching ridge, the root zone, and the tilled land, and a lower one more conductive, that is the untilled soil (see for more details Innocenti et al., 2024a). The accumulation of water in this second layer (about 30 cm below the ground level) was confirmed by the piezometers (the black rectangles in Figure 2).

Moisture sensors data (not presented here for brevity; refer to Innocenti et al., 2024b for more details) showed a higher percentage of VWC at depths of 30-40 in the high ridge and at depths of 20 cm in the low ridge. This is consistent with piezometer readings and identify a different distribution of irrigation water between the two mulch ridge heights. It is important to note that the ERTs at time T_0 (Figure 2a) clearly show that the three experimental fields have rather different characteristics from each other. The soil tillage and the creation of the mulch ridge led to the formation of non-homogeneous and uneven fields. Consequently, the water distribution in the subsoil, and thus the results of the time-lapse analysis are influenced by this initial condition. The results shown in Figure 2 highlight that the two-wings irrigation system is not able to distribute water evenly across the entire area. On the contrary, irrigation tends to favour the central area at the expense of the lateral zones, and over time, the irrigation water is not retained in the root zone but bypasses this level completely, moving to deeper layers where water accumulation occurs, as confirmed by piezometer P3. At time T_6, preferential pathways of surface water flows are observed, especially at point "A," through which water can reach deeper levels. The results also show that BRA3a+ leads to an excessive accumulation of water below the root zone, while BRA3a- offers better water supply to the root system, causing less water waste.

Having Diviner2000 data at each time Ti, for the BRA3a+ plot was possible to reconstruct the relationship between VWC, and electrical conductivity (EC) from ERT. It is shown in the graph in Figure 3. It shows together data for the high ridge (dark colours) and the low ridge (light colours) at each time of acquisition (different colours). The two datasets are in a perfect agreement. This was expected, because the correlation between VWC and EC is site-specific and should not depend on ridge height. Moreover, a concordance between the VWC and EC can be observed: when the first increases, the last increases too and vice versa. Using the obtained regression law, it is possible to convert the EC tomographies into VWC ones, and thus visualize the variation of the water content in the subsoil, as shown as an example, in Figure 3 for four selected times (T_0, T_1, T_3, and T_6).

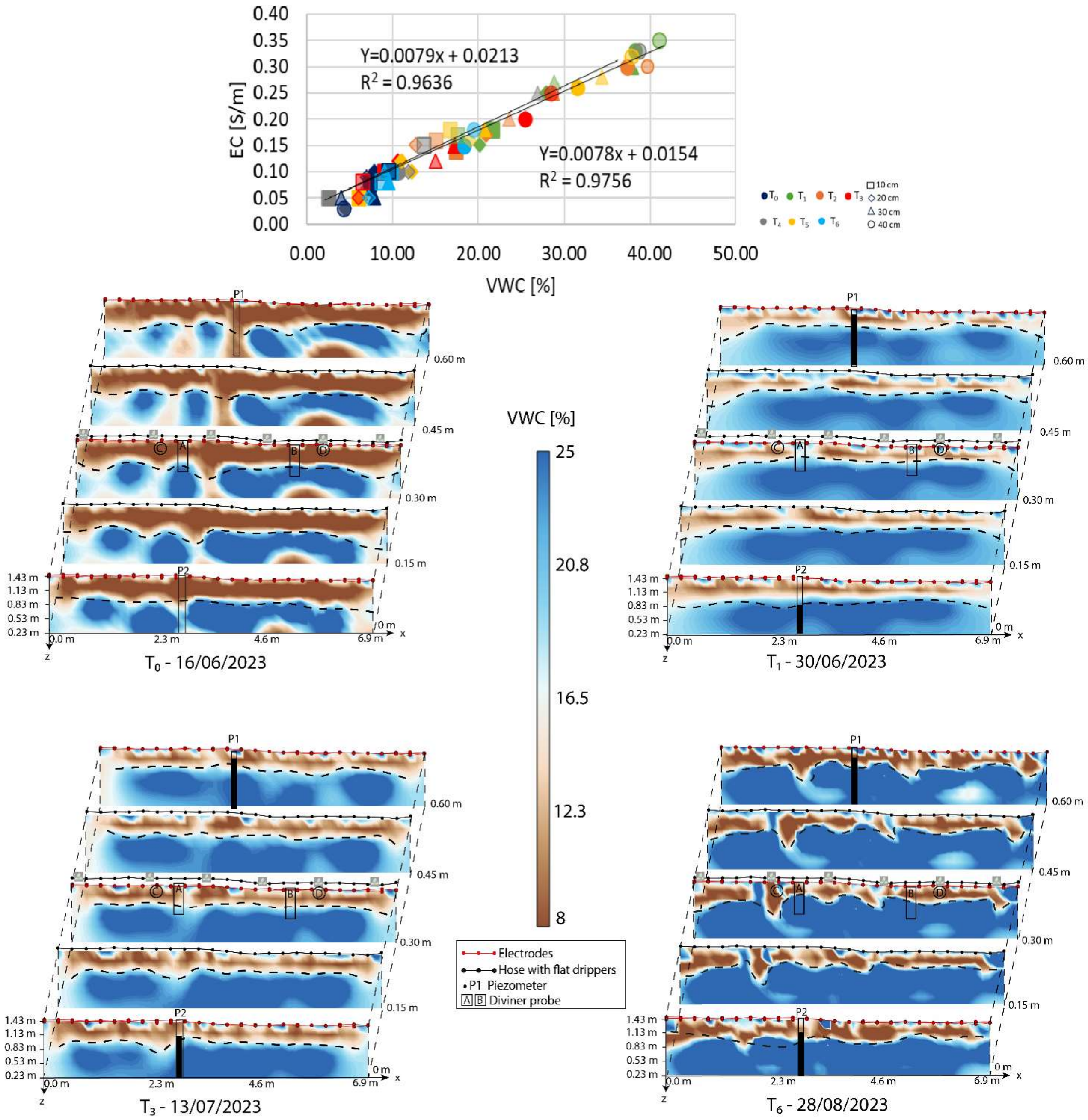

Fig. 3 – a) graph represents the relationship between the VWC recorded by the Diviner2000 probe and the EC derived from the ERT models for the high and low ridge. The symbols (squares, triangles, rhombuses, circles) represent the various acquisition depths. The colours represent the different acquisition times: the high ridge data are represented with dark colours, the low ridge data with light colours. b-e) represent the subsoil VWC distribution at time T_0, T_1, T_3, and T_6. The dashed black line represents the level of the water table.

Conclusions

This study was conducted to evaluate the effectiveness of two- and three-wings drip irrigation systems associated with mulch cover. The data shows the ineffectiveness of the two-wings system (BRA2a), while satisfactory results are achieved with BRA3a- (three-wings system with the same water flow as BRA2a) and BRA3a+ (three-wings system with the highest water flow). In particular, the BRA3a- system shows that the same amount of water as BRA2a, distributed by three wings instead of two, leads to a greater concentration of water in the root zone over time, slowly draining downward. In contrast, the BRA3a+ system distributes water uniformly like BRA3a-, but the amount introduced is excessive, causing the soil to remain above field capacity and draining a lot of water downward. The tests, in addition to considering which system was optimal, also evaluated the effectiveness of the mulch ridge, leading to the conclusion that during the summer period, when rainfall is less frequent or absent, the presence of a much lower ridge is much more effective as it allows irrigation water to be retained by the root system, avoiding excessive drainage.

Finally, having VWC data from direct measures, it is possible to reconstruct the site-specific law that link together VWC and EC, and it is possible to convert the ERTs into VWC tomographies.

References

Acosta J.A., Gabarrón M., Martínez-Segura M., Martínez-Martínez S., Faz Á., Pérez-Pastor A., Gómez-López M.D., Zornoza R.; 2022: Soil water content prediction using electrical resistivity tomography (ert) in mediterranean tree orchard soils. Sensors, 22, 1365.

Arshad I.; 2020: Importance of drip irrigation system installation and management-a review. Psm biological research, 5, 22–29.644

Chartzoulakis K., Bertaki M.; 2015: Sustainable water management in agriculture under climate change. Agriculture and Agricultural Science Procedia, 4, 88–98.684.

Ciani L., Patrizi G., Innocenti A., Fanti R., Pazzi V.; 2024: Considerations on the electrode spacing to electrode diameter ratio in electrical resistivity tomography (ert): an operational approach. IEEE Transactions on Instrumentation and Measurement.

Innocenti A., Pazzi V., Napoli M., Fanti R., Orlandini S.; 2024a: Assessing the efficiency of the irrigation system in a horticulture field through time-lapse electrical resistivity tomography. Irrigation Science, 1–15.

Innocenti A., Pazzi V., Napoli M., Ciampalini R., Orlandini S., Fanti R.; 2024b: Electrical resistivity tomography: A reliable tool to monitor the efficiency of different irrigation systems in horticulture field. Journal of Applied Geophysics, 230, 105527.

Luo X., Li C., Lin N., Wang N., Chu X., Feng H., Chen H.; 2023: Plastic film-mulched ridges and straw-mulched furrows increase soil carbon sequestration and net ecosystem economic benefit in a wheat-maize rotation. Agriculture, Ecosystems & Environment, 344, 108311.

Ratke R.F., Zuffo A.M., Steiner F., Aguilera J.G., de Godoy M.L., Gava R., … &Gonzales, H.H.S.; 2023: Can soil moisture and crop production be influenced by different cropping systems?. AgriEngineering, 5, 112–126.

Vanella D., Ramírez-Cuesta J. M., Sacco A., Longo-Minnolo G., Cirelli G. L., & Consoli S.; 2021: Electrical resistivity imaging for monitoring soil water motion patterns under different drip irrigation scenarios. Irrigation Science, 39(1), 145-157.

Wanniarachchi S., Sarukkalige R.; 2022: A review on evapotranspiration estimation in agricultural water management: Past, present, and future. Hydrology, 9(7), 123.

Zhang W., Dong A., Liu F., Niu W., & Siddique K. H.; 2022: Effect of film mulching on crop yield and water use efficiency in drip irrigation systems: A meta-analysis. Soil and tillage Research, 221, 105392.

Corresponding author: agnese.innocenti@unifi.it